Simple beam model for the shear failure of interfaces

F. Raischel,[1,*] F. Kun,[1,2] and H. J. Herrmann[1]
[1]*ICP, University of Stuttgart, Pfaffenwaldring 27, D-70569 Stuttgart, Germany*
[2]*Department of Theoretical Physics, University of Debrecen, P.O. Box 5, H-4010 Debrecen, Hungary*
(Received 3 February 2005; published 19 October 2005)

We propose a model for the shear failure of a glued interface between two solid blocks. We model the interface as an array of elastic beams which experience stretching and bending under shear load and break if the two deformation modes exceed randomly distributed breaking thresholds. The two breaking modes can be independent or combined in the form of a von Mises–type breaking criterion. Assuming global load sharing following the beam breaking, we obtain analytically the macroscopic constitutive behavior of the system and describe the microscopic process of the progressive failure of the interface. We work out an efficient simulation technique which allows for the study of large systems. The limiting case of very localized interaction of surface elements is explored by computer simulations.

DOI: 10.1103/PhysRevE.72.046126 PACS number(s): 62.20.Mk, 02.50.−r, 05.90.+m, 81.40.Np

I. INTRODUCTION

Solid blocks are often joined together by welding or gluing of the interfaces which are expected to sustain various types of external loads. When an elastic interface is subjected to an increasing load applied uniformly in the perpendicular direction, in the early stage of the failure process cracks nucleate randomly along the interface. Due to the heterogeneous microscopic properties of the glue, these cracks can remain stable under increasing load, which results in a progressive damage of the interface. This gradual softening process is followed by the localization of damage which leads then to the global failure of the interface and separation of the two solid blocks.

Interfacial failure plays a crucial role in fiber reinforced composites, which are constructed by embedding fibers in a matrix material [1]. Composites are often used as structural components since they have very good mass specific properties; i.e., they provide high strength with a relatively low mass, preserving this property even under extreme conditions. The mechanical performance of composites is mainly determined by the characteristic quantities of the constituents (fiber and matrix) and by the fabrication process which controls the material's microstructure, the formation of damage prior to applications, and the properties of the fiber-matrix interface. In many cases the reinforcement is a unidirectional arrangement of long fibers resulting in highly anisotropic mechanical properties; i.e., in the direction of the fiber axis the composite exhibits high strength and fracture toughness since the load is mainly carried by fibers. However, in the perpendicular direction the load bearing capacity is provided solely by the matrix material. Hence the dominant failure mechanism of unidirectional composites perpendicular to the fibers' direction is shear. Failure here occurs mainly due to the debonding of the fiber-matrix interface.

Since disordered properties of the glue play a crucial role in the failure of interfaces, most of the theoretical studies in this field rely on discrete models [2,3] which are able to capture heterogeneities and can account for the complicated interaction of nucleated cracks. The progressive failure of glued interfaces under a uniform load perpendicular to the interface has recently been studied by means of fiber bundle models [4–11]. Several aspects of the failure process have been revealed such as the macroscopic constitutive behavior, the distribution of avalanches of simultaneously failing glue, and the structure of failed glue regions [12]. Considering a hierarchical scheme for the load redistribution following fiber failure, a cascading mechanism was proposed for the softening interface in Refs. [13,14]. The roughness of the crack front propagating between two rigid plates due to an opening load was studied in the framework of the fuse model. The microcrack nucleation ahead the main crack and the structure of the damaged zone were analyzed in detail [15]. The shear failure of an interface between two rigid blocks has very recently been investigated by discretizing the interface in terms of springs. It was shown that shear failure of the interface occurs as a first-order phase transition [16].

In the present paper we study the shear failure of the glued interface connecting two solid blocks in the framework of a novel type of model. In our model the interface is discretized in terms of elastic beams which can be elongated and bent when exposed to shear load. Breaking of a beam is caused by two breaking modes—i.e., stretching and bending—characterized by randomly distributed threshold values. The two breaking modes can be either independent or combined in terms of a von Mises–type breaking criterion [17]. Assuming a long-range interaction among the beams, we obtained the full analytic solution of the model for the macroscopic response of the interface and for the microscopic process of failure. We show that the presence of two breaking modes lowers the critical stress and strain of the material without changing the statistics of bursts of simultaneously failing elements with respect to the case of a single breaking mode. The coupling of breaking modes results in further reduction of the strength of the interface. We demonstrate that varying the relative importance of the two breaking modes the macroscopic response of the interface can be tuned over a broad range. The limiting case of a very local-

*Electronic address: raischel@ica1.uni-stuttgart.de

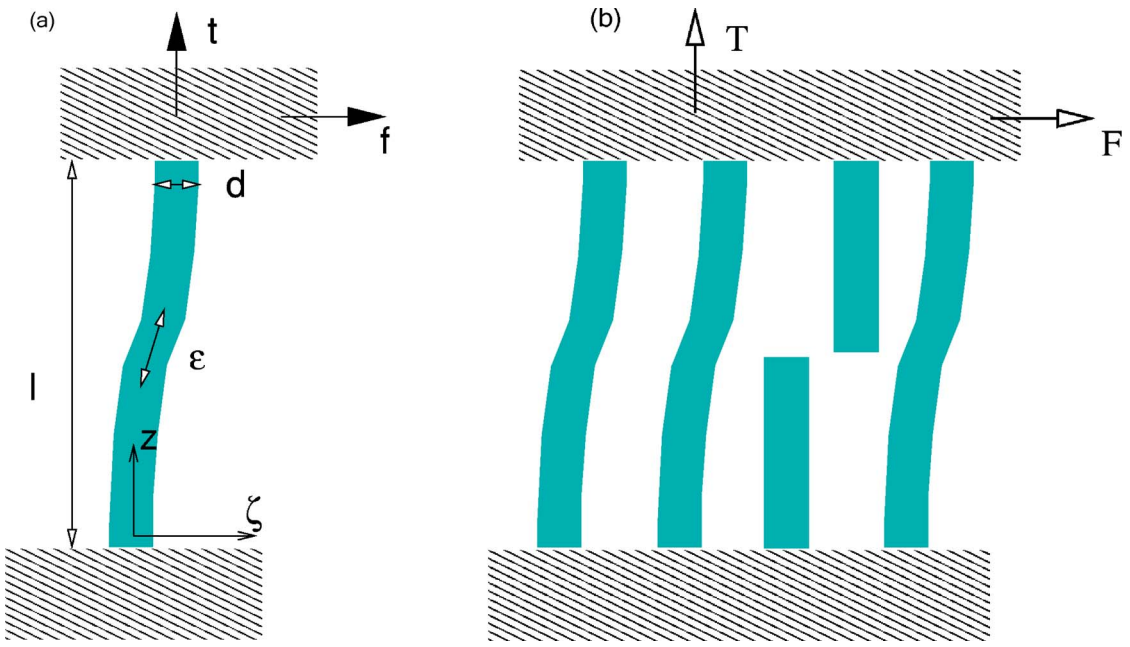

FIG. 1. (Color online) (a) Shearing of a single beam between two rigid plates. Since the distance l between the plates is kept constant, the beam experiences stretching and bending deformation, with longitudinal t and shear f forces. (b) Shearing of an array of beams, with the corresponding forces. In the case shown, one beam is broken.

ized interaction of beams is also considered. We determine the constitutive behavior and the distribution of avalanches of breaking beams for the case when beams interact solely with their nearest and next-nearest neighbors in a square lattice. An effective simulation technique is worked out which makes it possible to study systems of large size.

II. PROPERTIES OF THE MODEL

In our model we represent the glued interface of two solid blocks as an ensemble of parallel beams connecting the two surfaces. First, we derive an analytical description of a single beam of quadratic cross section clamped at both ends and sheared by an external force f; see Fig. 1(a). The shearing is exerted in such a way that the distance l between the two clamping planes is kept constant. Consequently, the beam experiences not only a torque m, but also a normal force t due to the elongation Δl, which is characterized by the longitudinal strain $\epsilon=\Delta l/l$.

We derive the form of the deflection curve of the beam, as well as the magnitude of the tension force. It is necessary to introduce some approximations so that the model can be incorporated into the simulation code in a sensible way. Following the procedure outlined, e.g., in [18], we solve the differential equation for the beam deflection $\zeta(z)$ under the influence of the lateral force f and a given stretching force t. We then solve self-consistently for $t(f)$, with t being the result of the longitudinal elongation.

The governing differential equation for the bending situation depicted in Fig. 1(a) can be cast in the form

$$\zeta'''(z) - \frac{t}{EI}\zeta'(z) = -\frac{f}{EI}, \tag{1}$$

with boundary conditions

$$\zeta(0) = 0,$$

$$\zeta'(0) = 0,$$

$$\zeta''(l/2) = 0. \tag{2}$$

Here, E denotes the modulus of elasticity and I is the moment of inertia for bending of the beam. For a beam of rectangular cross section, we have $I=d^4/12$, where d is the side length. Let us briefly motivate this ansatz by stating that the second derivative $\zeta''(z)$ is proportional to the torque on the beam, so consequently it needs to vanish at the beam half-length $l/2$. Accordingly, the third derivative $\zeta'''(z)$ is proportional to the shearing force exerted on the beam; hence, it constitutes a term of the balance equation (1). The first derivative term with $\zeta'(z)$ denotes the projection of the tension force t. Due to the clamping, the deflection and its first derivative must vanish at the end $z=0$. The formula for the bending moment m is

$$m = -EI\zeta''(z). \tag{3}$$

The solution $\zeta(z)$ for vanishing t can be obtained as [19]

$$\zeta(z) = \frac{fz^2}{12EI}(3l - 2z), \tag{4}$$

from which we can calculate the elongation

$$\Delta l = \int_0^l dz\sqrt{1 + \zeta'^2(z)} - l \approx \frac{1}{2}\int_0^l \zeta'^2 dz. \tag{5}$$

It follows from the above equation

$$t = ES\frac{\Delta l}{l} = ES\epsilon, \tag{6}$$

where $S=d^2$ is the beam cross-section area. The first-order solution for $t(f)$ reads as

$$t \approx \frac{l^4 S}{240EI^2} f^2. \tag{7}$$

From a computational point of view, a formulation of bending and stretching in terms of the longitudinal strain ϵ is more suitable than using the lateral force f. For that, we only need to replace $m(f)$ by $m(\epsilon)$, which yields

$$m(\epsilon) \approx \frac{fl}{2} = \sqrt{\frac{5}{12}}\frac{Ed^4}{l}\sqrt{\epsilon}, \tag{8}$$

with

$$\epsilon = \frac{t}{ES} = \frac{3l^4}{5E^2d^8} f^2. \tag{9}$$

Using ϵ as an independent variable enables us to make comparisons to the simple case of fiber bundle models [4,5,7,8,20,21] where the elements can have solely stretching deformation. In the model we represent the interface as an ensemble of parallel beams connecting the surface of two rigid blocks [see Fig. 1(b)]. The beams are assumed to have identical geometrical extensions (length l and side length d) and linearly elastic behavior characterized by the Young modulus E. In order to capture the failure of the interface in the model, the beams are assumed to break when their deformation exceeds a certain threshold value. As has been shown above, under shear loading of the interface beams suffer stretching and bending deformation resulting in two modes of breaking. The two breaking modes can be considered to be independent or combined in the form of a von Mises–type breaking criterion. The strength of beams is characterized by the two threshold values of stretching ϵ_1 and bending ϵ_2 a beam can withstand. The breaking thresholds are assumed to be randomly distributed variables of the joint probability distribution function (PDF) $p(\epsilon_1,\epsilon_2)$. The randomness of the breaking thresholds is supposed to represent the disorder of the interface material.

After breaking of a beam the excess load has to be redistributed over the remaining intact elements. Coupling to the rigid plates ensures that all the beams have the same deformation giving rise to global load sharing (GLS); i.e., the load is equally shared by all the elements—and stress concentration in the vicinity of failed beams cannot occur. If one of the interfaces has a certain compliance, the load redistribution following the breaking of beams becomes localized. This case has recently been studied for an external load imposed perpendicular to the interface [16].

In the present study we are mainly interested in the macroscopic response of the interface under shear loading and the process of the progressive failure of interface elements. The global load sharing of beams enables us to obtain closed analytic results for the constitutive behavior of the system for both independent and coupled breaking modes. We examine by computer simulations the statistics of simultaneously failing elements. The limiting case of the very localized interaction of interface elements is explored by computer simulations.

III. CONSTITUTIVE BEHAVIOR

Assuming global load sharing for the redistribution of load after the failure of beams, the most important characteristic quantities of the interface can be obtained in closed analytic form.

Breaking of the beam is caused by two breaking modes—i.e., stretching and bending, which can be either independent or coupled by an empirical breaking criterion. Assuming that the two breaking modes are independent, a beam breaks if either the longitudinal stress t or the bending moment m exceeds the corresponding breaking threshold. Since the longitudinal stress t and the bending moment m acting on a beam can easily be expressed as functions of the longitudinal deformation ϵ, the breaking conditions can be formulated in a transparent way in terms of ϵ. To describe the relative importance of the breaking modes, we assign to each beam two breaking thresholds $\epsilon_1^i, \epsilon_2^i$, $i=1,\ldots,N$, where N denotes the number of beams. The threshold values ϵ_1 and ϵ_2 are randomly distributed according to a joint probability density function $p(\epsilon_1,\epsilon_2)$ between lower and upper bounds $\epsilon_1^{\min}, \epsilon_1^{\max}$ and $\epsilon_2^{\min}, \epsilon_2^{\max}$, respectively. The density function needs to obey the normalization condition

$$\int_{\epsilon_2^{\min}}^{\epsilon_2^{\max}} d\epsilon_2 \int_{\epsilon_1^{\min}}^{\epsilon_1^{\max}} d\epsilon_1 p(\epsilon_1,\epsilon_2) = 1. \tag{10}$$

A. *OR* breaking rule

First, we provide a general formulation of the failure of a bundle of beams. We allow for two independent breaking modes of a beam that are functions f and g of the longitudinal deformation ϵ. Later on this case will be called the *OR* breaking rule. A single beam breaks if either its stretching or bending deformation exceeds the respective breaking threshold ϵ_1 or ϵ_2; i.e., failure occurs if

$$\frac{f(\epsilon)}{\epsilon_1} \geqslant 1 \tag{11}$$

or

$$\frac{g(\epsilon)}{\epsilon_2} \geqslant 1, \tag{12}$$

where Eqs. (11) and (12) describe the stretching and bending breaking modes, respectively. The functions $f(\epsilon)$ and $g(\epsilon)$ are called failure functions, for which the only restriction is that they be monotonic functions of ϵ. For our specific case of elastic beams the failure functions can be determined from Eqs. (6) and (8) as

$$f(\epsilon) = \epsilon, \quad g(\epsilon) = a\sqrt{\epsilon}, \tag{13}$$

where a is a constant and the value of the Young modulus E is set to 1.

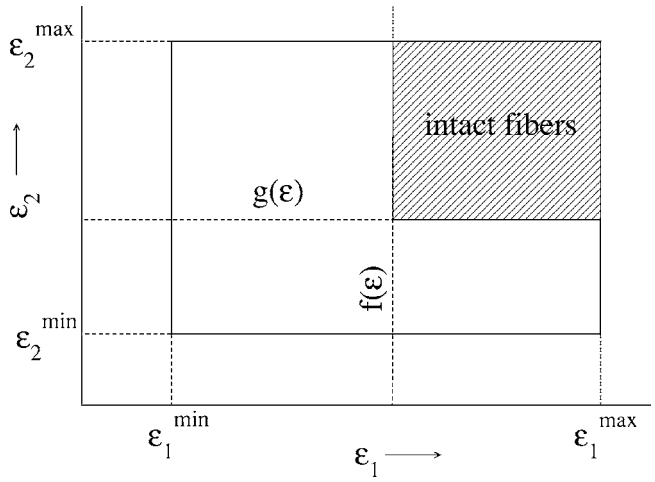

FIG. 2. Plane of breaking thresholds (ϵ_1, ϵ_2). The point of intersection of $f(\epsilon)$ and $g(\epsilon)$ determines the fraction of remaining beams.

In the plane of breaking thresholds each point (ϵ_1, ϵ_2) represents a beam. For each value of ϵ those beams which survived the externally imposed deformation are situated in the area $f(\epsilon) \leqslant \epsilon_1 \leqslant \epsilon_1^{\max}$ and $g(\epsilon) \leqslant \epsilon_2 \leqslant \epsilon_2^{\max}$, as is illustrated in Fig. 2. Hence, the fraction of intact beams, N_{intact}/N, at a given value of ϵ can be obtained by integrating the density function over the shaded area in Fig. 2:

$$\frac{N_{\text{intact}}}{N} = \int_{g(\epsilon)}^{\epsilon_2^{\max}} d\epsilon_2 \int_{f(\epsilon)}^{\epsilon_1^{\max}} d\epsilon_1 p(\epsilon_1, \epsilon_2). \tag{14}$$

Due to the global load sharing, deformation and stress of the beams are the same everywhere along the interface. Consequently, the macroscopic elastic behavior of the system can be obtained by multiplying the load of a single beam, $\sigma^{(1)} = \epsilon$ ($E=1$ is taken), by the fraction of intact elements, Eq. (14):

$$\sigma = \epsilon \int_{g(\epsilon)}^{\epsilon_2^{\max}} d\epsilon_2 \int_{f(\epsilon)}^{\epsilon_1^{\max}} d\epsilon_1 p(\epsilon_1, \epsilon_2). \tag{15}$$

Assuming that the breaking thresholds, characterizing the relative importance of the two breaking modes, are independently distributed, the joint PDF can be factorized as

$$p(\epsilon_1, \epsilon_2) = p_1(\epsilon_1) p_2(\epsilon_2). \tag{16}$$

Introducing the cumulative distribution functions (CDF's) as

$$P_1(\epsilon_1) = \int_{\epsilon_1^{\min}}^{\epsilon_1} p_1(\epsilon_1') d\epsilon_1', \quad P_2(\epsilon_2) = \int_{\epsilon_2^{\min}}^{\epsilon_2} p_2(\epsilon_2') d\epsilon_2', \tag{17}$$

we can rewrite Eq. (15) as

$$\sigma = \epsilon \int_{g(\epsilon)}^{\epsilon_2^{\max}} d\epsilon_2 p_2(\epsilon_2) \int_{f(\epsilon)}^{\epsilon_1^{\max}} d\epsilon_1 p_1(\epsilon_1)$$
$$= \epsilon [1 - P_2(g(\epsilon))][1 - P_1(f(\epsilon))]. \tag{18}$$

This is the general formula for the constitutive behavior of a beam bundle with two breaking modes applying the *OR* criterion. In the constitutive equation $1 - P_1(f(\epsilon))$ and $1 - P_2(g(\epsilon))$ are the fraction of those beams whose threshold value for bending and stretching is larger than $g(\epsilon)$ and $f(\epsilon)$, respectively. It follows from the structure of Eq. (18) that the existence of two breaking modes leads to a reduction of the strength of the material; both the critical stress and strain take smaller values compared to the case of a single breaking mode applied in simple fiber bundle models [4–11].

Considering the special case of two uniform distributions for the breaking thresholds in the intervals $[\epsilon_1^{\min}, \epsilon_1^{\max}]$ and $[\epsilon_2^{\min}, \epsilon_2^{\max}]$, respectively, we can derive the specific form of Eq. (18) by noting that

$$p(\epsilon_1) = \frac{1}{\epsilon_1^{\max} - \epsilon_1^{\min}}, \quad p(\epsilon_2) = \frac{1}{\epsilon_2^{\max} - \epsilon_2^{\min}}. \tag{19}$$

After calculating the cumulative distributions, the final result follows as

$$\sigma = \epsilon \frac{[\epsilon_1^{\max} - f(\epsilon)][\epsilon_2^{\max} - g(\epsilon)]}{[\epsilon_1^{\max} - \epsilon_1^{\min}][\epsilon_2^{\max} - \epsilon_2^{\min}]}. \tag{20}$$

More specifically, if the distributions have equal boundaries $[0, 1]$ and substituting the failure functions f and g from Eq. (13), the constitutive equation takes the form

$$\sigma = \epsilon [1 - \epsilon][1 - a\sqrt{\epsilon}]. \tag{21}$$

B. von Mises–type breaking rule

We now address the more complicated case that the two breaking modes are coupled by a von Mises–type breaking criterion: a single beam breaks if its strain ϵ fulfills the condition [17]

$$\left(\frac{f(\epsilon)}{\epsilon_1}\right)^2 + \frac{g(\epsilon)}{\epsilon_2} \geqslant 1. \tag{22}$$

This algebraic condition can be geometrically represented as is illustrated in Fig. 3. In the plane of the failure thresholds, ϵ_1, ϵ_2, the beams that survive a load ϵ are bounded by the maximum values $\epsilon_1^{\max}, \epsilon_2^{\max}$ and the hyperbola defined by Eq. (22). Calculating the intersection points a and b defined in Fig. 3, which are found to be

$$a = f(\epsilon) \left(\frac{\epsilon_2^{\max}}{\epsilon_2^{\max} - g(\epsilon)}\right)^{1/2},$$

$$b = \frac{g(\epsilon)(\epsilon_1^{\max})^2}{(\epsilon_1^{\max})^2 - f^2(\epsilon)}, \tag{23}$$

the fraction of surviving beams can be expressed as

$$\frac{N_{\text{intact}}}{N} = \int_a^{\epsilon_1^{\max}} d\epsilon_1 \int_{\tilde{\epsilon}_2(\epsilon_1, \epsilon)}^{\epsilon_2^{\max}} d\epsilon_2 p(\epsilon_1, \epsilon_2), \tag{24}$$

with the integration limit

$$\tilde{\epsilon}_2(\epsilon_1, \epsilon) = \frac{\epsilon_1^2 g(\epsilon)}{\epsilon_1^2 - f^2(\epsilon)}. \tag{25}$$

The constitutive behavior in this case is therefore given by

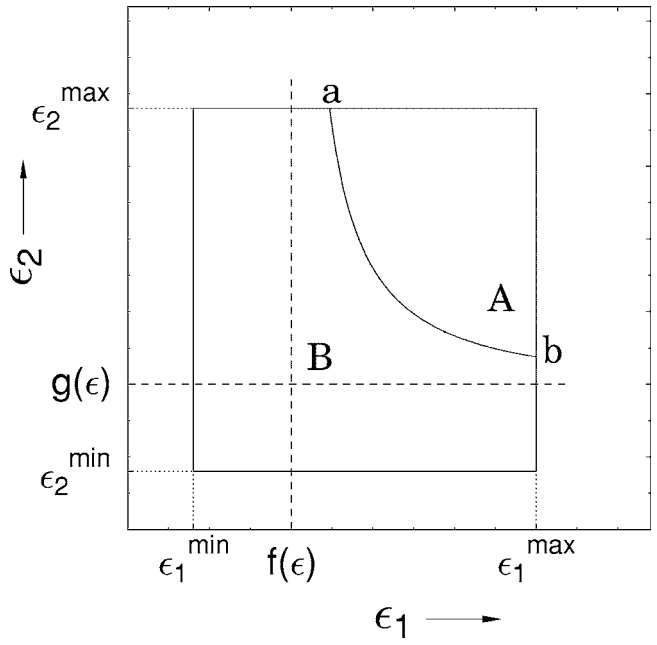

FIG. 3. Intact beams in the plane of the failure thresholds, ϵ_1, ϵ_2, for a given strain ϵ, if breaking is determined by the von Mises criterion. The values a and b are defined as the intersections between the curve of the breaking condition, Eq. (22), and the maximum values $\epsilon_1^{\max}$ and $\epsilon_2^{\max}$, respectively. The shaded region labeled A denotes the intact beams; the shaded region B represents the additionally failing beams that would be intact in the case of the *OR* criterion.

$$\sigma = \epsilon \int_a^{\epsilon_1^{\max}} d\epsilon_1 \int_{\tilde{\epsilon}_2(\epsilon_1,\epsilon)}^{\epsilon_2^{\max}} d\epsilon_2 p(\epsilon_1, \epsilon_2). \tag{26}$$

We would like to emphasize that assuming independence of the breaking thresholds the joint distribution factorizes $p(\epsilon_1, \epsilon_2) = p_1(\epsilon_1) p_2(\epsilon_2)$, but the integrals in Eq. (26) over the two variables cannot be performed independently. Still, the integral in Eq. (26) can be evaluated analytically for a broad class of disorder distributions. As an example, we again consider two homogeneous distributions, Eqs. (19), over the interval [0, 1] along with the failure functions, Eqs. (13). Setting the Young modulus and the parameter $E=1=a$, the integrals yield

$$\sigma = \epsilon \frac{1}{2} \left[\left(2 - 2\sqrt{\epsilon} + \epsilon^{3/2} \ln \frac{1+\epsilon}{1-\epsilon} \right) - \epsilon^{3/2} \left(2 \sqrt{\frac{1-\sqrt{\epsilon}}{\epsilon}} + \ln \frac{1+\sqrt{1-\sqrt{\epsilon}}}{1-\sqrt{1-\sqrt{\epsilon}}} \right) \right]. \tag{27}$$

Even for the simplest case of uniformly distributed breaking thresholds, the constitutive equation takes a rather complex form. It is important to note that the coupling of the two breaking modes gives rise to a higher amount of broken beams compared to the *OR* criterion. In Fig. 3 the beams which break due to the coupling of the two breaking modes fall in the area labeled by B.

IV. COMPUTER SIMULATIONS

In order to determine the behavior of the system for complicated disorder distributions and explore the microscopic failure process of the sheared interface, it is necessary to work out a computer simulation technique. In the model we consider an ensemble of N beams arranged on a square lattice. Two breaking thresholds $\epsilon_1^i, \epsilon_2^i$ are assigned to each beam $i (i=1, \ldots, N)$ of the bundle from the joint probability distribution $p(\epsilon_1, \epsilon_2)$. For the *OR* breaking rule, the failure of a beam is caused either by stretching or bending depending on which one of the conditions, Eq. (11) or (12), is fulfilled at a lower value of the external load. This way an effective breaking threshold ϵ_c^i can be defined for the beams as

$$\epsilon_c^i = \min(f^{-1}(\epsilon_1^i), g^{-1}(\epsilon_2^i)), \quad i = 1, \ldots, N, \tag{28}$$

where f^{-1} and g^{-1} denote the inverse of f and g, respectively. A beam i breaks during the loading process of the interface when the load on it exceeds its effective breaking threshold ϵ_c^i. For the case of the von Mises–type breaking criterion, Eq. (22), the effective breaking threshold ϵ_c^i of beam i can be obtained as the solution of the algebraic equation

$$\left(\frac{f(\epsilon_c^i)}{\epsilon_1^i} \right)^2 + \frac{g(\epsilon_c^i)}{\epsilon_2^i} = 1, \quad i = 1, \ldots, N. \tag{29}$$

Although for the specific case of the functions f, g given by Eqs. (11) and (12) the above equation can be converted to a fourth-order polynomial and solved analytically, this solution turns out to be impractical, especially since the numerical evaluation of the solution is too slow. We therefore solve Eq. (29) numerically by means of a modified Newton root finding scheme, where we make use of the fact that the solution has the lower bound 0.

In the case of global load sharing, the load and deformation of beams is everywhere the same along the interface, which implies that beams break in the increasing order of their effective breaking thresholds. In the simulation, after determining ϵ_c^i for each beam, they are sorted in increasing order. Quasistatic loading of the beam bundle is performed by increasing the external load to break only a single element. Due to the subsequent load redistribution on the intact beams, the failure of a beam may trigger an avalanche of breaking beams. This process has to be iterated until the avalanche stops or it leads to catastrophic failure at the critical stress and strain. Under strain-controlled loading conditions, however, the load of the beams is always determined by their deformation so that there is no load redistribution and avalanche activity.

In Fig. 4 the analytic results of Sec. III on the constitutive behavior, Eqs. (21) and (27), are compared to the corresponding results of computer simulations. As a reference, we also plotted the constitutive behavior of a bundle of fibers where the fibers fail solely due to simple stretching [4–11]. It can be seen in the figure that the simulation results are in perfect agreement with the analytical predictions. It is important to note that the presence of two breaking modes substantially reduces the critical stress σ_c and strain ϵ_c (σ and ϵ values of the maximum of the constitutive curves) with respect to the case when failure of elements occurs solely un-

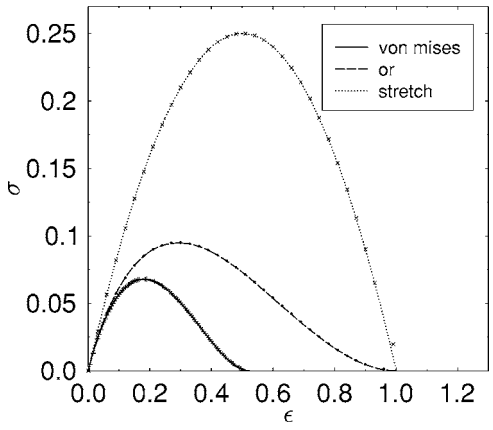

FIG. 4. Constitutive behavior of a bundle of beams with two breaking modes in a strain-controlled simulation of $N=4\times10^5$ beams, under the *OR* (dashed line), von Mises—type (solid line), and pure stretching breaking (dotted line) criteria. The random failure thresholds for the breaking modes of each beam are sampled from uniform distribution between [0, 1]. The points marked with ·, +, and × denote the respective theoretical results, Eqs. (21) and (27), and $\sigma=\epsilon(1-\epsilon)$ for the pure stretching case. The constants E and a are set to unity here.

der stretching. Since one of the failure functions $g(\epsilon)$ is nonlinear, the shape of the constitutive curve $\sigma(\epsilon)$ also changes, especially in the post-peak regime. The coupling of the two breaking modes in the form of the von Mises criterion gives rise to further reduction of the strength of the interface.

V. PROGRESSIVE FAILURE OF THE INTERFACE

During the quasistatic loading process of an interface, avalanches of simultaneously failing beams occur. Inside an avalanche, however, the beams can break under different breaking modes when the *OR* criterion is considered or the breaking can be dominated by one of the breaking modes in the coupled case of the von Mises–type criterion. Hence, it is an important question how the fraction of beams breaking due to a specific breaking mode (stretching or bending) varies during the course of loading of the interface.

For the *OR* criterion, those beams break, for instance, under bending—i.e., under mode g defined by Eq. (12), whose effective breaking threshold ϵ_c^i is determined by $g^{-1}(\epsilon_2^i)$ in Eq. (28) so that the inequality holds:

$$g^{-1}(\epsilon_2^i) < f^{-1}(\epsilon_1^i). \tag{30}$$

In the plane of breaking thresholds $\{\epsilon_1,\epsilon_2\}$ the region of beams which fulfill the above condition is indicated by shading in Fig. 5. The fraction of beams $\mathcal{B}_g(\epsilon)$ breaking under mode g up to the macroscopically imposed deformation ϵ can be obtained by integrating the probability distribution $p(\epsilon_1,\epsilon_2)$ over the shaded area in Fig. 5. Taking into account the fact that the intersection points a,b defined in Fig. 5 may in general lie outside the rectangle $(\epsilon_1^{\min},\epsilon_1^{\max},\epsilon_2^{\max},\epsilon_2^{\min})$ and adjusting the integral limits accordingly, we arrive at the following formula for the fraction of fibers breaking under mode g as a function of the deformation ϵ:

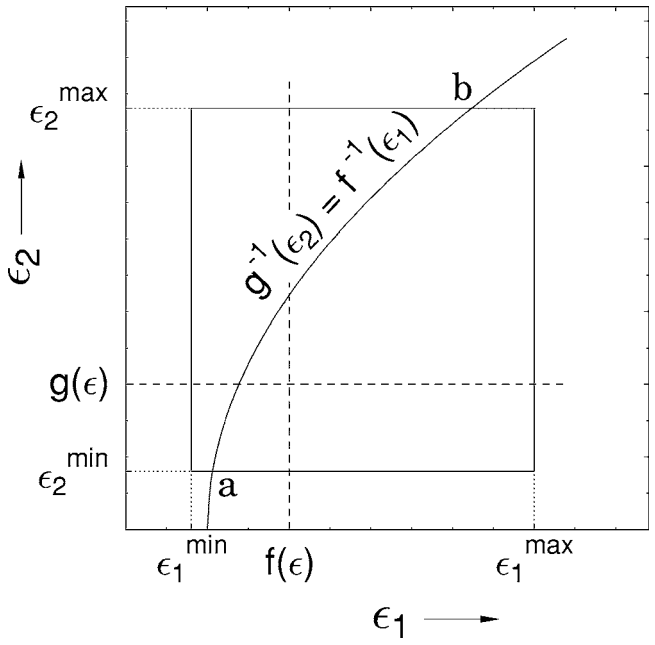

FIG. 5. The beams that break due to mode g fall in the shaded region. The labels a and b mark the abscissas of the intersection points of the curve $g^{-1}(\epsilon_2)=f^{-1}(\epsilon_1)$ with the lines $\epsilon_2=\epsilon_2^{\min}$ and $\epsilon_2=\epsilon_2^{\max}$, respectively.

$$\begin{aligned}\mathcal{B}_g(\epsilon) = &\int_{\max(\epsilon_1^{\min},a)}^{\min(f(\epsilon),b)} d\epsilon_1 \int_{\epsilon_2^{\min}}^{g(f^{-1}(\epsilon_1))} d\epsilon_2 p(\epsilon_1,\epsilon_2) \\ &+ \int_{\min(f(\epsilon),b)}^{f(\epsilon)} d\epsilon_1 \int_{\epsilon_2^{\min}}^{\epsilon_2^{\max}} d\epsilon_2 p(\epsilon_1,\epsilon_2) \\ &+ \int_{f(\epsilon)}^{\epsilon_1^{\max}} d\epsilon_1 \int_{\epsilon_2^{\min}}^{g(\epsilon)} d\epsilon_2 p(\epsilon_1,\epsilon_2).\end{aligned} \tag{31}$$

It should be noted that the second integral vanishes unless $b<\epsilon_1^{\max}$. The total fraction of beams breaking under mode g during the entire course of the loading can be obtained by substituting $\epsilon=\epsilon^{\max}$ in the above formulas, where $\epsilon^{\max}$ denotes the deformation at the breaking of the last beam.

In order to study the effect of the disorder distribution $p(\epsilon_1,\epsilon_2)$ of beams on the relative importance of the two breaking modes and on the progressive failure of the interface, we considered independently distributed breaking thresholds ϵ_1,ϵ_2 both with a Weibull distribution

$$p_b(\epsilon_b) = \frac{m_b}{\lambda_b}\left(\frac{\epsilon_b}{\lambda_b}\right)^{m_b-1} \exp\left[-\left(\frac{\epsilon_b}{\lambda_b}\right)^{m_b}\right], \tag{32}$$

where index b can take values 1 and 2. The exponents m_1 and m_2 determine the amount of disorder in the system for stretching and bending, respectively—i.e., the width of the distributions, Eq. (32)—while the values of λ_1 and λ_2 set the average strength of beams for the two breaking modes. Computer simulations were performed in the framework of global load sharing by setting equal values for the shape parameters $m_1=m_2$ and fixing the value of $\lambda_1=1$ of the stretching mode, while varying λ_2 of the bending mode.

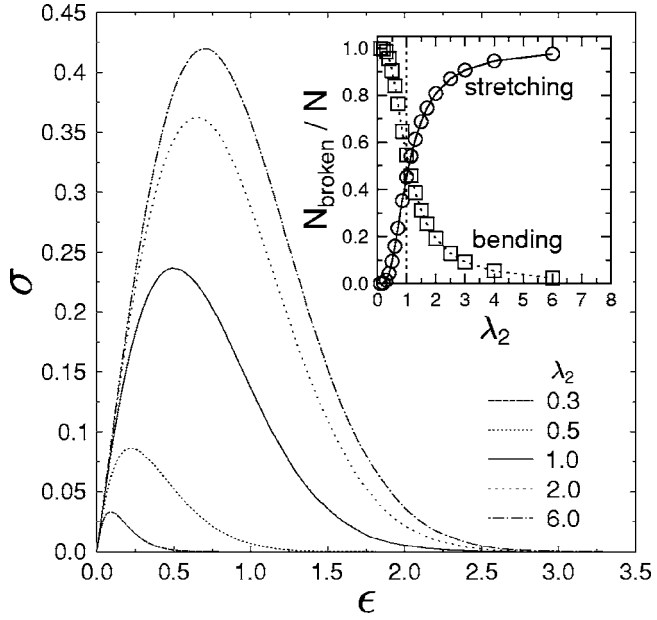

FIG. 6. Constitutive behavior of a bundle of $N=90\,000$ beams using the *OR* criterion. The parameter values $\lambda_1=1.0$ (stretching), $m_1=m_2=2$ were fixed, while λ_2 corresponding to the bending mode was shifted. Inset: fraction of beams breaking by stretching and bending as a function of λ_2.

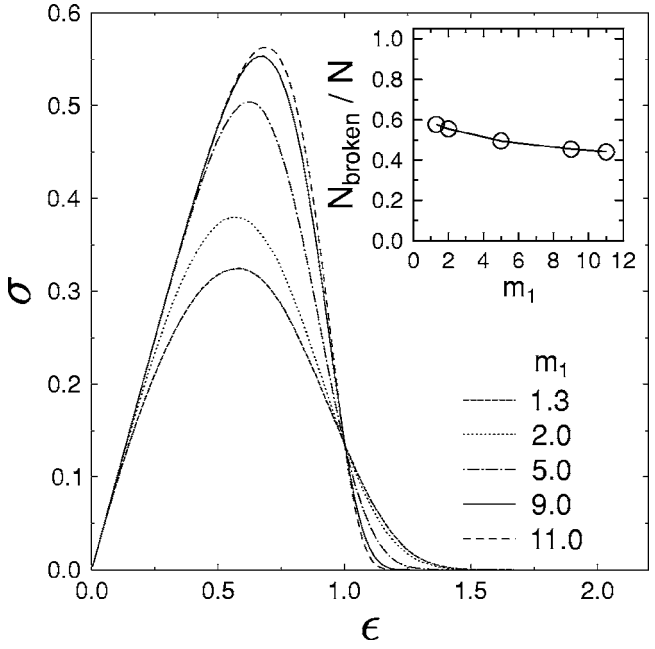

FIG. 7. Constitutive behavior for different values of the shape parameter m_1 of stretching. Strain-controlled simulation of $N=90\,000$ beams with failure due to the *OR* criterion, fixing the parameters $\lambda_1=\lambda_2=1.0$ and $m_2=2$. Inset: total fraction of beams broken under mode g during the course of loading.

The total fraction of beams breaking by stretching and bending using the *OR* breaking rule is presented in Fig. 6. Increasing λ_2 of the bending mode, the beams become more resistant against bending so that the stretching mode starts to dominate the breaking of beams, which is indicated by the increasing fraction of stretching failure in the figure. In the limiting case of $\lambda_2 \gg \lambda_1$ the beams solely break under stretching. Decreasing λ_2 has the opposite effect: more and more beams fail due to bending, while the fraction of beams breaking by the stretching mode tends to zero. It is interesting to note that varying the relative importance of the two failure modes gives also rise to a change of the macroscopic constitutive behavior of the system. Figure 6 illustrates that shifting the strength distributions of beams the functional form of the constitutive behavior remains the same; however, the values of the critical stress and strain vary in a relatively broad range.

The same analysis can also be performed by fixing the values λ_1 and λ_2 and changing the relative width of the two distributions by varying one of the Weibull shape parameters m. We find it convenient to shift m_1, the shape parameter of the stretching mode, instead of m_2. It can be observed in Fig. 7 that for this choice of the scale parameters λ, the value of the critical strain hardly changes; however, the critical stress nearly doubles as compared to Fig. 6.

Although the effect on the final fraction of beams broken by each mode (see the inset of Fig. 7) is not as pronounced as for shifting λ, we should also consider the fraction of fibers broken up to a value of ϵ during the loading process (Fig. 8). It should be noted that the end points of the respective curves in Fig. 8 are just the final fraction numbers in Fig. 7, but the curves show a strong spread for intermediate values of ϵ. This demonstrates that changing the amount of disorder in the breaking thresholds strongly influences the process of damaging of the interface.

We apply the methods outlined in the previous paragraphs to the von Mises case. Obviously, Eq. (22) does not allow for a strict separation of the two modes. However, the breaking of a beam at a certain value ϵ_c is dominated by stretching if

$$\left(\frac{f(\epsilon)}{\epsilon_1}\right)^2 > \frac{g(\epsilon)}{\epsilon_2}. \tag{33}$$

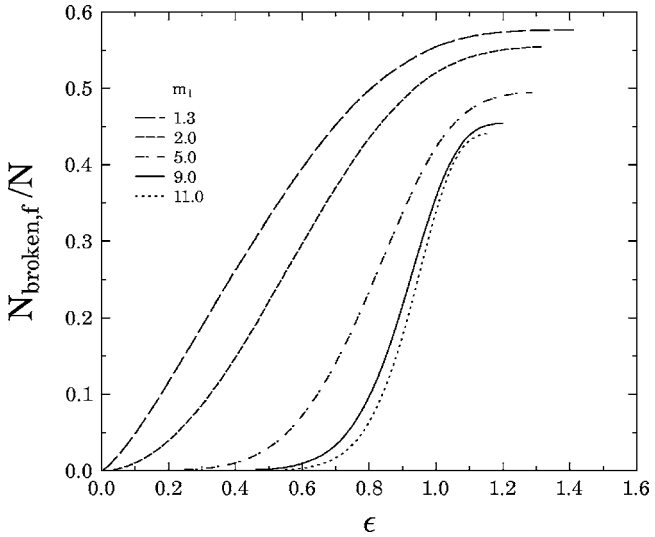

FIG. 8. Fraction of fibers broken by the stretching mode as a function of ϵ for different values of the corresponding shape parameter m_1. Strain-controlled simulation with failure due to the *OR* criterion, $N=90\,000$, $\lambda_1=\lambda_2=1.0$, $m_2=9$.

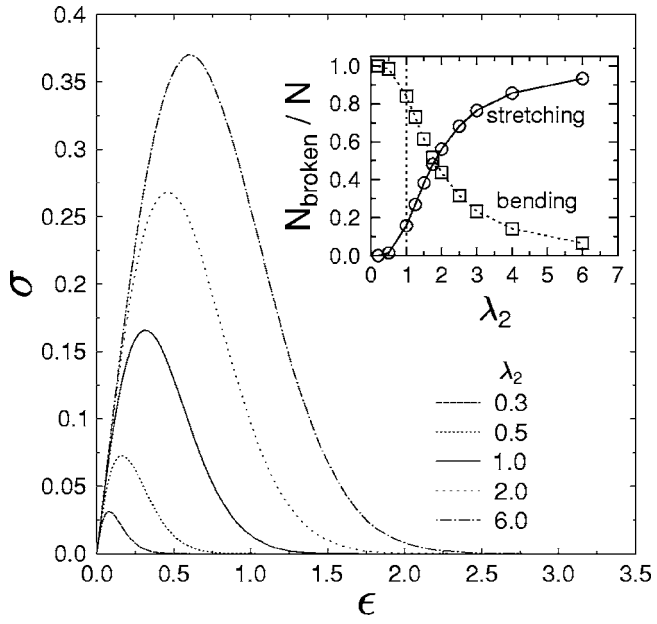

FIG. 9. Constitutive behavior for different values of the bending scale parameter λ_2. Strain-controlled simulation with the von Mises criterion, $N=90\,000$, $\lambda_1=1.0$, $m_1=m_2=2$. The inset presents the fraction of beams whose failure was dominated by the stretching or bending mode.

With the previous prescriptions for the failure functions, Eqs. (13), we again find a massive influence on the constitutive behavior and the final number of broken beams; see Fig. 9. The inset of Fig. 9 demonstrates that a crossover between stretching and bending preponderance occurs also in the von Mises case.

VI. AVALANCHE STATISTICS

The stress-controlled loading of the glued interface is accompanied by avalanches of simultaneously failing elements. The avalanche activity can be characterized by the distribution $D(\Delta)$ of burst sizes Δ defined as the number of beam breakings triggered by the failure of a single beam. In the framework of simple fiber bundle models, it has been shown analytically that global load sharing gives rise to a power-law distribution of avalanche sizes for a very broad class of disorder distributions of materials strength [6,22]:

$$D(\Delta) \propto \Delta^{-\delta}, \tag{34}$$

with an universal exponent $\delta=5/2$.

In the previous sections we have shown that in our model the interplay of the two breaking modes results in a complex failure mechanism on the microscopic level, which is strongly affected by the distributions of the breaking thresholds. In order to investigate the bursts of breaking beams we performed stress-controlled simulations on large systems ($N=10^4\cdots16\times10^6$) with both the *OR* and von Mises–type breaking criterion. In Fig. 10 the simulation results are compared to the avalanche size distribution of a simple fiber bundle model where failure occurs solely due to stretching [6–9,22]. In all the cases the avalanche size distributions can be fitted by a power law over three orders of magnitude. The best fit exponent of $\delta=2.56\pm0.08$ was derived from the system of size $N=16\times10^6$ beams, with an average taken over 100 samples. The size of the largest avalanche in the inset of Fig. 10 proved to be proportional to the system size. It can be concluded that the beam model belongs to the same universality class as the fiber bundle model [6–9,22].

VII. LOCAL LOAD SHARING

During the failure of interfaces, stress localization is known to occur in the vicinity of failed regions, which results in correlated growth and coalescence of cracks. In our model this effect can be captured by a localized interaction of the interface elements, which naturally occurs when the two solid blocks are not perfectly rigid [12]. For simplicity, in our model solely the extremal case of very localized interactions is considered; i.e., after breaking of a beam in the square lattice, the load is redistributed equally on its nearest

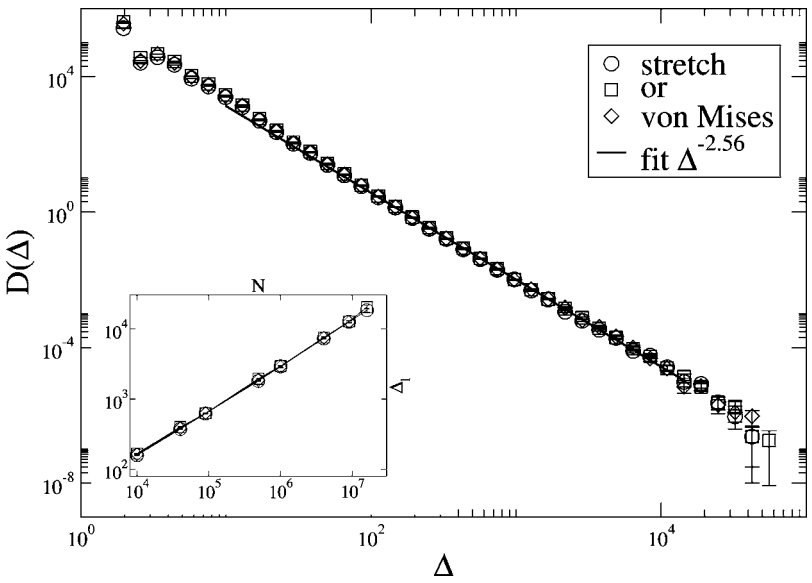

FIG. 10. Avalanche size distribution $D(\Delta)$ for pure stretching of a fiber bundle and the two beam breaking conditions for system sizes $N=16\times10^6$, averaged over 100 runs. A fit with the best result $D\propto\Delta^{-2.56}$ over almost four decades is provided. The inset shows the dependence of the largest avalanche Δ_l on the system size for the three cases. Again, no difference is found.

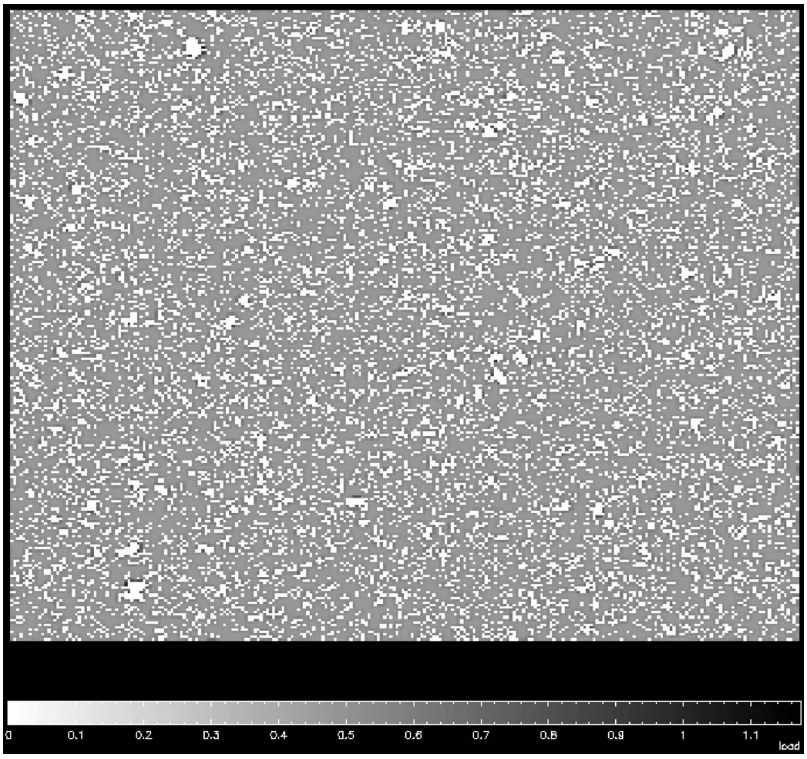

FIG. 11. Snapshot of a LLS system at the last stable configuration. The color coding represents the load per beam, with broken beams carrying a vanishing load. The system size is $L=100$.

and next-nearest intact neighbors. This localized load sharing (LLS) results in growing failed regions (cracks) with high stress concentration along their perimeter [7,12,23]. Figure 11 shows the last stable configuration of a beam lattice preceding global failure, which was obtained using the *OR* criterion for beam breaking. Due to the stress concentration around cracks, the onset of a catastrophic avalanche occurs at lower external loads making the macroscopic response of the interface more brittle compared to the case of global load sharing [7,12,23].

As for global load sharing, we shift the relative importance of the two breaking modes by changing their threshold distributions and record the influence on microscopic and macroscopic system properties. We consider here the *OR* criterion and use two Weibull distributions with parameters λ_1,λ_2 and m_1,m_2, where the indices 1 and 2 denote the stretching and bending mode, respectively. Varying λ_2 for a fixed λ_1, we find a considerable influence on the constitutive properties, as Fig. 12 illustrates.

We investigated also the distribution of avalanche sizes for LLS, Fig. 13, where we vary the scale parameter λ_2 of the bending mode g. We find merely a shifting to different amplitudes, but no considerable effect on the shape of the distribution function, which is similar to the one reported in [7]. In comparison to the global load sharing case, we should note that large avalanches cannot occur and the functional form of the curves can be approximated by a power law with an exponent higher than for GLS in agreement with Refs. [6,22,23].

VIII. CONCLUDING REMARKS

Fiber bundle models have been applied to describe various aspects of the failure of heterogeneous interfaces. However, fibers can sustain solely elongation and hence cannot account for more complex deformation states of interface elements, which naturally occurs under shear loading. We constructed a model for the shear failure of the glued interface of two solid blocks. In the model the interface is discretized in terms of elastic beams which experience stretching and bending deformation under shear. Breaking of a beam can be caused by both deformations, resulting in two failure modes. The mechanical strength of beam elements is characterized by the two threshold values of stretching and bending the beam can withstand. The beams are assumed to have identical elastic properties; the heterogeneous microstructure is represented by the disorder distribution of the

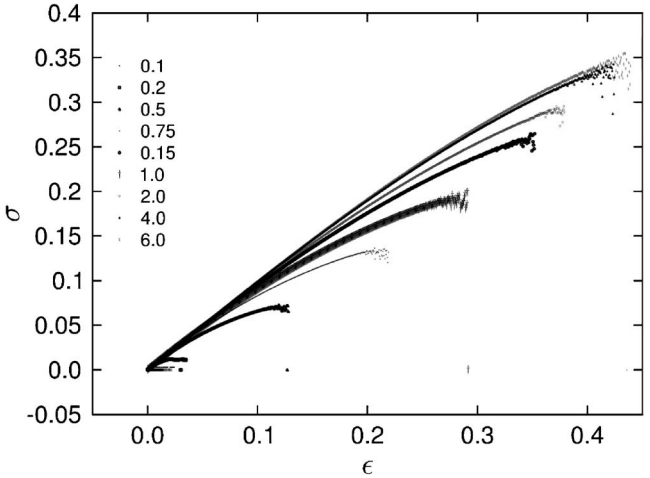

FIG. 12. Constitutive curves in the LLS case, shifting λ_2 and keeping the parameters $\lambda_1=1.0$ and $m_1=m_2=2$ fixed. Stress-controlled simulation of $N=10\,000$ fibers averaged over 300 runs.

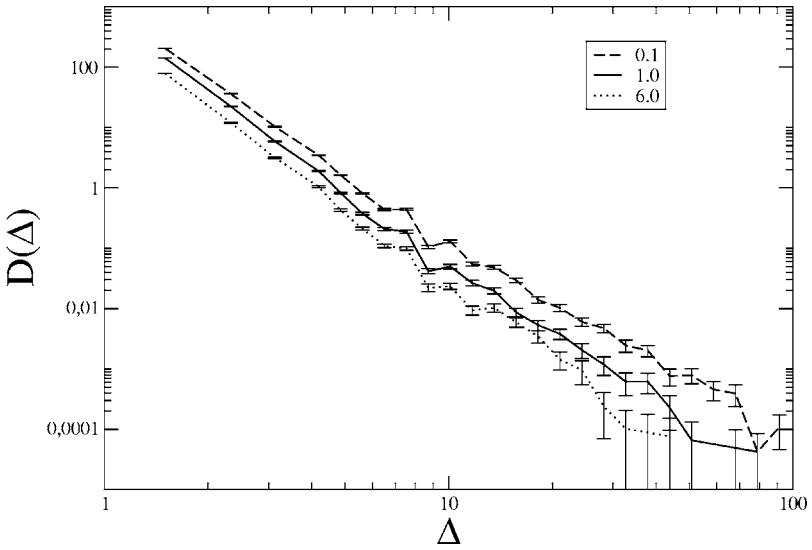

FIG. 13. Distribution of avalanche sizes for LLS for three values of λ_2, with $\lambda_1=1$ and $m_1=m_2=2$ fixed. Simulations were performed using the *OR* criterion for a bundle of 10 000 beams averaged over 300 runs.

breaking thresholds. In the model we assume that the two solid blocks are perfectly rigid which results in a global load redistribution over the intact beams following the breaking events.

We presented a detailed study of the macroscopic response and the progressive damaging of the interface under quasistatic loading. Making use of the global load sharing of intact beams, we obtained the analytic solution of the model for the constitutive behavior and the amount of damage during the course of loading. In order to explore the microscopic process of damaging we worked out an efficient simulation technique which enables us to study large systems. We demonstrated that the disorder distribution and the relative importance of the two failure modes have a substantial effect on both the microscopic damage process and the macroscopic constitutive behavior of the interface. Varying its parameters, the model provides a broad spectrum of material behaviors. Simulations showed that the failure of the interface proceeds in bursts of simultaneously breaking beams. The distribution of burst sizes follows power-law behavior with an exponent equal to the one of simple fiber bundles. Under stress-controlled loading conditions, the macroscopic failure of the interface occurs analogously to phase transitions, where our beam model proved to be in the same universality class as the equal-load-sharing fiber bundle model [7,21,24]. We showed that the localized interaction of beams leads to a more brittle behavior of the interface, which implies a more abrupt transition at the critical load.

Beam models have been successfully applied to study the fracture of cohesive frictional materials where cracks usually form along the grain-grain interface. Beam elements proved to give a satisfactory description of the interfacial failure of grains and the emerging microbehavior and macrobehavior of materials [25]. Our beam model presented here provides a more realistic description of the interface of macroscopic solid bodies than the simple fiber bundle model and is applicable to more complex loading situations. Experiments on the shear failure of glued interfaces are rather limited, especially on the microscopic mechanism of the progressive damage, which hinders the direct comparison of our theoretical results to experimental findings. Our work in this direction is in progress.

ACKNOWLEDGMENTS

We wish to thank F. Wittel for useful discussions. This work was supported by the Collaborative Research Center SFB381. F.K. acknowledges financial support of Research Contract Nos. NKFP-3A/043/04, OTKA M041537, and T049209 and of the György Békési Foundation of the Hungarian Academy of Sciences.

[1] R. W. Cahn, P. Haasen, and E. J. Kramer, *Structure and Properties of Composites* (VCH-Verlag, Weinheim, 1993).
[2] *Statistical Models for the Fracture of Disordered Media*, edited by H. J. Herrmann and S. Roux, *Random Materials and Processes* (Elsevier, Amsterdam, 1990).
[3] *Continuous and Discontinuous Modeling of Cohesive-Frictional Materials*, edited by P. Vermeer *et al.*, *Lecture Notes in Physics* (Springer, New York, 2000).
[4] H. E. Daniels, Proc. R. Soc. London, Ser. A **183**, 405 (1945).
[5] D. Sornette, J. Phys. A **22**, L243 (1989).
[6] M. Kloster, A. Hansen, and P. C. Hemmer, Phys. Rev. E **56**, 2615 (1997).
[7] R. C. Hidalgo, Y. Moreno, F. Kun, and H. J. Herrmann, Phys. Rev. E **65**, 046148 (2002).
[8] R. C. Hidalgo, F. Kun, and H. J. Herrmann, Phys. Rev. E **64**, 066122 (2001).
[9] Y. Moreno, J. B. Gomez, and A. F. Pacheco, Phys. Rev. Lett. **85**, 2865 (2000).
[10] S. Pradhan and B. K. Chakrabarti, Phys. Rev. E **67**, 046124 (2003).
[11] P. Bhattacharyya, S. Pradhan, and B. K. Chakrabarti, Phys. Rev. E **67**, 046122 (2003).

[12] G. G. Batrouni, A. Hansen, and J. Schmittbuhl, Phys. Rev. E **65**, 036126 (2002).
[13] A. Delaplace, S. Roux, and G. Pijaudier-Callot, Int. J. Solids Struct. **36**, 1403 (1999).
[14] S. Roux, A. Delaplace, and G. Pijaudier-Cabot, Physica A **270**, 35 (1999).
[15] S. Zapperi, H. J. Herrmann, and S. Roux, Eur. Phys. J. B **17**, 131 (2000).
[16] J. Knudsen and A. R. Massih, e-print cond-mat/0410280.
[17] H. J. Herrmann, A. Hansen, and S. Roux, Phys. Rev. B **39**, 637 (1989).
[18] L. D. Landau and E. M. Lifschitz, *Theory of Elasticity*, 3rd ed. (Butterworths-Heinemann, London, 1986).
[19] *Dubbel Taschenbuch für den Maschinenbau*, 20th ed. edited by W. Beitz and K.-H. Grote (Springer-Verlag, New York, 2001).
[20] D. Sornette, J. Phys. (Paris) **50**, 745 (1989).
[21] S. Pradhan and B. K. Chakrabarti, Int. J. Mod. Phys. B **17**, 5565 (2003).
[22] P. C. Hemmer and A. Hansen, J. Appl. Mech. **59**, 909 (1992).
[23] A. Hansen and P. C. Hemmer, Phys. Lett. A **184**, 394 (1994).
[24] J. V. Andersen, D. Sornette, and K. T. Leung, Phys. Rev. Lett. **78**, 2140 (1997).
[25] G. A. D' Addetta, F. Kun, E. Ramm, and H. J. Herrmann, in *Continuous and Discontinuous Modelling of Cohesive-Frictional Materials*, edited by P. Vermeer *et al.*, *Lecture Notes in Physics* (Springer-Verlag, Berlin, 2001).